

Research Article



Biocompatibility and bioactive potential of the NeoMTA Plus endodontic bioceramic-based sealer

Roberto Alameda Hoshino ¹, Mateus Machado Delfino ¹,
Guilherme Ferreira da Silva ², Juliane Maria Guerreiro-Tanomaru ¹,
Mário Tanomaru-Filho ¹, Estela Sasso-Cerri ³, Paulo Sérgio Cerri ^{3*}

¹Department of Restorative Dentistry, Dental School, São Paulo State University (UNESP), Araraquara, SP, Brazil

²Pro-Rectorate of Research and Post-graduation, School of Dentistry, Universidade Sagrado Coração (USC), Bauru, SP, Brazil

³Department of Morphology, Genetics, Orthodontics and Pediatric Dentistry, Laboratory of Histology and Embryology, Dental School, São Paulo State University (UNESP), Araraquara, SP, Brazil



Received: Apr 3, 2020

Revised: May 9, 2020

Accepted: May 11, 2020

Hoshino RA, Delfino MM, Silva GF, Guerreiro-Tanomaru JM, Tanomaru-Filho M, Sasso-Cerri E, Cerri PS

*Correspondence to

Paulo Sérgio Cerri, DDS, MS, PhD

Professor, Laboratory of Histology and Embryology, Dental School, São Paulo State University (UNESP), Rua Humaitá, 1680, Araraquara, SP 14.801-903, Brazil.
E-mail: paulo.cerri@unesp.br

Copyright © 2021. The Korean Academy of Conservative Dentistry

This is an Open Access article distributed under the terms of the Creative Commons Attribution Non-Commercial License (<https://creativecommons.org/licenses/by-nc/4.0/>) which permits unrestricted non-commercial use, distribution, and reproduction in any medium, provided the original work is properly cited.

Funding

Financial support provided by FAPESP (2016/09264-9) and CNPq (Brazil).

Conflict of Interest

No potential conflict of interest relevant to this article was reported.

Author Contributions

Conceptualization: Cerri PS, Tanomaru-Filho M; Formal analysis: Hoshino RA, Delfino MM,

ABSTRACT

Objectives: This study evaluated the biocompatibility and bioactive potential of NeoMTA Plus mixed as a root canal sealer in comparison with MTA Fillapex.

Materials and Methods: Polyethylene tubes filled with NeoMTA Plus ($n = 20$), MTA Fillapex ($n = 20$), or nothing (control group, CG; $n = 20$) were inserted into the connective tissue in the dorsal subcutaneous layer of rats. After 7, 15, 30 and 60 days, the specimens were processed for paraffin embedding. The capsule thickness, collagen content, and number of inflammatory cells (ICs) and interleukin-6 (IL-6) immunolabeled cells were measured. von Kossa-positive structures were evaluated and unstained sections were analyzed under polarized light. Two-way analysis of variance was performed, followed by the *post hoc* Tukey test ($p \leq 0.05$).

Results: At 7 days, the capsules around NeoMTA Plus and MTA Fillapex had more ICs and IL-6-immunostained cells than the CG. However, at 60 days, there was no significant difference in the IC number between NeoMTA Plus and the CG ($p = 0.1137$) or the MTA Fillapex group ($p = 0.4062$), although a greater number of IL-6-immunostained cells was observed in the MTA Fillapex group ($p = 0.0353$). From 7 to 60 days, the capsule thickness of the NeoMTA Plus and MTA Fillapex specimens significantly decreased, concomitantly with an increase in the collagen content. The capsules around root canal sealers showed positivity to the von Kossa stain and birefringent structures.

Conclusions: The NeoMTA Plus root canal sealer is biocompatible and exhibits bioactive potential.

Keywords: Bioactive potential; Biocompatibility; Immunohistochemistry; Inflammatory reaction; Interleukin-6

INTRODUCTION

Bioceramic-based materials are highly attractive in dentistry due to their favorable biological and physicochemical properties [1]. Tricalcium silicate-based materials have been widely studied,

Cerri PS, Sasso-Cerri E; Funding acquisition: Cerri PS; Investigation: Hoshino RA, Silva GF, Guerreiro-Tanomaru J; Methodology: Hoshino RA, Delfino MM; Supervision: Cerri PS; Writing - original draft: Hoshino RA, Delfino MM, Sasso-Cerri E, Cerri PS; Writing - review & editing: Hoshino RA, Delfino MM, Silva GF, Guerreiro-Tanomaru JM, Tanomaru-Filho M, Sasso-Cerri E, Cerri PS.

ORCID iDs

Roberto Alameda Hoshino 
<https://orcid.org/0000-0002-2123-3001>
Mateus Machado Delfino 
<https://orcid.org/0000-0002-6386-9200>
Guilherme Ferreira da Silva 
<https://orcid.org/0000-0002-8019-6714>
Juliane Maria Guerreiro-Tanomaru 
<https://orcid.org/0000-0003-0446-2037>
Mário Tanomaru-Filho 
<https://orcid.org/0000-0002-2574-4706>
Estela Sasso-Cerri 
<https://orcid.org/0000-0002-9148-3081>
Paulo Sérgio Cerri 
<https://orcid.org/0000-0001-5756-5828>

since these materials promote tissue repair, facilitating the formation of mineralized tissue [2,3]. Although mineral trioxide aggregate (MTA) is a biocompatible material that has been used for various applications such as furcation or root drilling treatment, apical microsurgery, retrofilling, pulp capping, pulpotomy, and root repair [4,5], it has some drawbacks [4]. MTA-based sealers have been developed due to the biocompatibility and bioactive properties of MTA. However, MTA can release some heavy metal components and exert a deleterious effect on tissues [6]. Therefore, calcium silicate-based sealers have been introduced.

New calcium silicate-based sealers contain mainly tricalcium and dicalcium silicate [2], with the addition of radiopacifying agents, tantalum oxide, and calcium tungstate. These materials are designated as bioactive since when they come into contact with biological fluids, they form an interfacial layer on the material surface, at the material/dentin interface, and in the dentinal tubules [7]. It has been suggested that this interfacial layer containing apatite crystals may reduce microleakage and increase the pushing force, improving adaptation and inducing remineralization [8]. NeoMTA Plus (Avalon Biomed Inc., Bradenton, FL, USA) is a bioactive material containing fine powdered tricalcium and dicalcium silicate, tantalite, calcium sulfate and silica, as stated by the manufacturer, with a short hardening time and no discoloration of dentin. Besides cement powder, NeoMTA Plus contains a water-based gel that yields a material with a consistency that varies depending on the powder-gel ratio that is mixed [5]. Thus, this material can be used with a thin consistency as a root canal sealer, whereas a thick mixture is indicated as a root-end filling material [9,10]. NeoMTA Plus mixed as a root canal sealer had a prolonged final setting time of around 315 minutes, although the release of calcium and hydroxyl ions was higher from this material than from MTA Plus [5]. In contrast, the setting time reported for NeoMTA Plus mixed as a repair material was around 67 minutes [11], showing that the proportion of the powder and gel has an important influence on the physical properties of NeoMTA Plus. An *in vitro* study evaluated the effect of thick NeoMTA Plus (repair material) on a Saos-2 cell culture and demonstrated that it induced mineralized nodule formation, suggesting its bioactive potential [12]. Cavities created in the femur and filled with NeoMTA Plus showed bone formation, indicating that this material stimulated tissue repair and may be bioactive [11]. However, the tissue response induced by the NeoMTA Plus root canal sealer has not yet been studied. The substantial difference in the setting time reported between NeoMTA Plus prepared as a repair material and NeoMTA Plus root canal sealer suggests the possibility that the powder/gel ratio could also affect the biological response to this calcium silicate.

Fillapex MTA (Angelus Dental Industry S/A, Lindóia, SP, Brazil) is an endodontic sealer containing approximately 13.2% tricalcium silicate [13], with the addition of natural resin, salicylate resin, bismuth oxide, silica nanoparticles, and pigments [14]. According to the manufacturer, the properties of MTA Fillapex include good radiopacity, good working time, and ease of handling [14]. As bismuth oxide inhibits cellular proliferation [15], this radiopacifier was replaced by calcium tungstate in an attempt to improve its biological properties. It has been demonstrated that MTA Fillapex with calcium tungstate exhibits a lengthy hardening time of around 637 minutes [16]. An *in vivo* study demonstrated that although MTA Fillapex initially promoted moderate inflammatory infiltration in the subcutaneous connective tissue, a decrease in interleukin-6 (IL-6), a pro-inflammatory cytokine, was observed over time. Moreover, the apoptotic index in the capsules around MTA Fillapex specimens was similar to that observed in the control specimens at 60 days, indicating that the structural integrity of the tissues was recovered [17].

Here, we analyzed the tissue response induced by NeoMTA Plus prepared as a root canal sealer compared to MTA Fillapex. Furthermore, the bioactivity of these endodontic sealers was also evaluated. The null hypothesis was that there would be no differences in biocompatibility and bioactive potential between NeoMTA Plus and MTA Fillapex.

MATERIALS AND METHODS

Experimental procedures

The present study was conducted in accordance with Brazilian national laws on animal use, and the experimental protocol was approved by the Ethical Committee for Animal Research of Dental School of Araraquara (CEUA #11/2017; São Paulo State University - UNESP, São Paulo, SP, Brazil).

Sixty adult male Holtzman rats (*Rattus norvegicus albinus*) were housed in polypropylene cages covered with a layer of white pine shavings with food (Guabi rat chow, Paulínia, SP, Brazil) and water *ad libitum*. The rats were kept in a room under standardized photoperiod (12 hours light/dark), temperature ($23^{\circ}\text{C} \pm 2^{\circ}\text{C}$) and humidity ($55\% \pm 10\%$).

The 60 rats were randomly separated into the following 3 groups, each containing 20 animals: the NeoMTA Plus group (Avalon Biomed Inc.), the MTA Fillapex group (Angelus Dental Industry S/A), and the control group (CG). In the CG, the polyethylene tubes were kept empty (without endodontic sealer). In each group, the animals were randomly distributed into 4 experimental periods: 7, 15, 30, and 60 days. Thus, 5 animals from each group were euthanized at each time point. Animals were sacrificed on day 7 in order to evaluate the degree of inflammatory reaction initially induced by endodontic sealers, while the endpoint of 60 days was chosen as a time point when it would be expected that these materials would have allowed the structural reorganization of tissue components, confirming their biocompatibility. The periods of 15 and 30 days were chosen as intermediary time points that help to understand the cascade of cellular events involved in the tissue response to the materials [17-20].

The sealers were manipulated inside a laminar flux chamber under aseptic conditions. NeoMTA Plus was manipulated using the ratio of 1 g per 350 μL of vehicle for root canal sealing, whereas for MTA Fillapex the 2 pastes were mixed in the same proportion (**Table 1**). After mixing, the sealers were inserted into sterilized polyethylene tubes (Embramed Indústria Comércio, São Paulo, SP, Brazil) measuring 10.0 mm length \times 1.0 mm internal diameter \times 1.6 mm external diameter.

The rats received by the ketamine hydrochloride (80 mg/kg body weight [bw]) through the intraperitoneal route and 8 mg/kg bw of xylazine hydrochloride using an insulin syringe and

Table 1. Manufacturers, chemical components, and proportions of the root canal sealers

| Root canal sealers | Manufacturer and chemical composition | Powder-liquid ratio |
|--------------------|---|---|
| NeoMTA Plus | <ul style="list-style-type: none"> Avalon Biomed Inc., Bradenton, FL, USA. Powder: Tricalcium silicate, dicalcium silicate, tantalum oxide, tricalcium aluminate and calcium sulphate. Liquid: water-based gel with thickener agents and water soluble polymers. | One scoop of powder (1 g) and 3 drops of water-based gel (350 μL) |
| MTA Fillapex | <ul style="list-style-type: none"> Angelus Dental Industry S/A, Lindóia, SP, Brazil. Paste: salicylate resin, diluting resin, natural resin, calcium tungstate, nanoparticulated silica, MTA, pigments. | Two pastes mixed with same proportion |

MTA, mineral trioxide aggregate.

needle. A trichotomy was made in the surgical area and a 1.0 cm-long incision with sterilized surgical scissors was performed in the dorsal skin, followed by divulsion of tissues to obtain a pocket. Each animal received 1 implant in a subcutaneous pocket with 1 of the evaluated materials or 1 empty polyethylene tube. The implants were maintained for 7, 15, 30, and 60 days. At each time point, 5 rats per group were killed by overdose of the anesthetic, and the implants with the surrounding tissues were subsequently removed and immersed in 4% formaldehyde solution.

Paraffin embedding procedures

The specimens were maintained for 48 hours in 4% formaldehyde buffered with 0.1 M sodium phosphate at a pH of 7.2. The specimens were dehydrated in graded series of ethanol, treated with xylene, and embedded in paraffin. Serial longitudinal sections (6 μm thick) were obtained using a microtome (Leica RM 2145 RTS; Leica Microsystem GmbH, Wetzlar, Germany). The histological description was performed in non-serial sections stained with Carazzi's hematoxylin and eosin (H&E). Moreover, in H&E-stained sections, the number of inflammatory cells (ICs) was quantified and the thickness of the capsules around the implants was measured. Immunohistochemical staining of the sections was performed to detect IL-6 and the number of immunostained cells was estimated. Birefringent collagen was quantified in the sections stained with picrosirius red. To evaluate the bioactive potential of materials, the von Kossa histochemical reaction was used to detect structures containing calcium, and unstained sections were observed under polarized light in the attempt to detect calcite deposits in the capsules.

The sections were analyzed using a light microscope (BX51; Olympus, Tokyo, Japan) with a digital camera (DP71; Olympus) and morphometric analyses were performed with help of an image analysis system (Image Pro-Express 6.0, Olympus). The analyses were performed by a calibrated and blinded examiner.

Morphological analysis and numerical density of ICs

The morphology and number of ICs in the capsules were analyzed in 3 H&E-stained non-serial sections per specimen. In each specimen, a field (0.09 mm^2) was captured in the central portion of the capsule in close juxtaposition to the tube opening, at $\times 695$. In these fields, the ICs (neutrophils, lymphocytes, macrophages, and plasma cells) were identified and counted. Afterwards, the numerical density of ICs was estimated in each specimen and the mean per group was calculated [17-19].

1. Capsule thickness

In each implant, the thickness of the capsules was estimated in 3 sections per specimen, with a minimal distance of 100 μm , stained with H&E. The images were captured at $\times 65$ magnification and the thickness was measured in the central portion, from the innermost surface until adjacent tissues, as previously described [17,20]. The capsule thickness in each specimen was obtained and the mean of the group was calculated at each time point.

2. IL-6 detection by immunohistochemistry

The slides containing dewaxed sections were placed in 0.001 M sodium citrate buffered at pH 6.0 and heated at 96°C–98°C for 20 minutes. After a cooling-off period, the slides were washed in phosphate-buffered saline at pH 7.3 and, then were immersed for 20 minutes in 5% hydrogen peroxide to inactivate the endogenous peroxidase. The sections were treated for 30 minutes with 2% bovine serum albumin (Sigma-Aldrich Chemie GmbH, Munich,

Germany) and incubated overnight at 4°C with mouse monoclonal anti-IL-6 antibody (Abcam Inc., Cambridge, MA, USA), diluted to 1:400. Subsequently, the sections were incubated with a labeled StreptAvidin-Biotin Kit (Universal Dako LSAB; Dako Inc., Carpinteria, CA, USA) for 1 hour. The sections were then treated with 3,3'-diaminobenzidine (Dako Inc.) for 2–3 minutes, washed with tap water and counterstained with hematoxylin. In the negative controls, the primary antibody was replaced by non-immune serum (Sigma-Aldrich Chemie GmbH).

The number of IL-6-immunostained cells (brown-yellow color) was computed in a standardized field (0.09 mm²). The number of immunostained cells was obtained in all specimens and periods. For each specimen, the number of immunopositive cells was obtained in the standardized field and, subsequently, the number of immunolabelled cells/mm² was estimated [17-20].

3. Collagen measurement

Collagen was quantified in the sections stained with 0.1% picosirius red solution and analyzed by polarized light microscopy. This analysis was performed in 3 sections from each specimen, with a minimal distance of 100 µm between the sections. The polarized images were captured at ×40 magnification with rigorously standardized parameters (light intensity, diaphragm aperture, condenser position and exposition time) and the birefringent material (*i.e.*, collagen) was estimated as previously described [21]. The hue definition considered in the birefringence was as follows: red/orange, 2–38 and 230–256; yellow, 39–51; and green, 52–128. The amount of collagen was represented by the percentage of birefringent areas of the total area (expressed in pixels) calculated by ImageJ® analysis software [21-23].

4. von Kossa histochemical reaction and unstained sections analyzed under polarized light
Two non-serial sections were analyzed using the von Kossa histochemical reaction and the sections were subsequently counterstained with picosirius red according to a previously described protocol [18,20,23]. Unstained sections were also analyzed under polarized illumination to investigate the presence of structures exhibiting birefringence in the capsules [23-25].

Statistical analysis

The statistical analysis was performed using GraphPad Prism 5.0 (Graph Pad Software Inc., San Diego, CA, USA). As the omnibus normality test (D'Agostino-Person) detected a normal distribution of the data, the values obtained were subjected to 2-way analysis of variance and the Tukey *post hoc* test. The significance level was set at $p \leq 0.05$.

RESULTS

Analyses of H&E-stained sections: morphological and quantitative findings

At 7 days, the capsules around the opening of polyethylene tubes were thick and exhibited an evident inflammatory infiltrate, but structural changes were not observed in the adjacent tissues (**Figure 1A-1C**). The analysis of the capsules revealed that the inflammatory infiltrate mainly contained macrophages and lymphocytes (**Figure 1D-1F**). At 15 days, the well-defined capsules showed ICs dispersed among some fibroblasts and blood vessels (**Figure 1G-1L**). The capsules of MTA Fillapex generally exhibited several material particles intermingled with ICs and fibroblasts (**Figure 1H**). In the CG, the capsules exhibited typical fibroblasts between collagen fibers, whereas the ICs were restricted mainly to portions next to the lumen of the

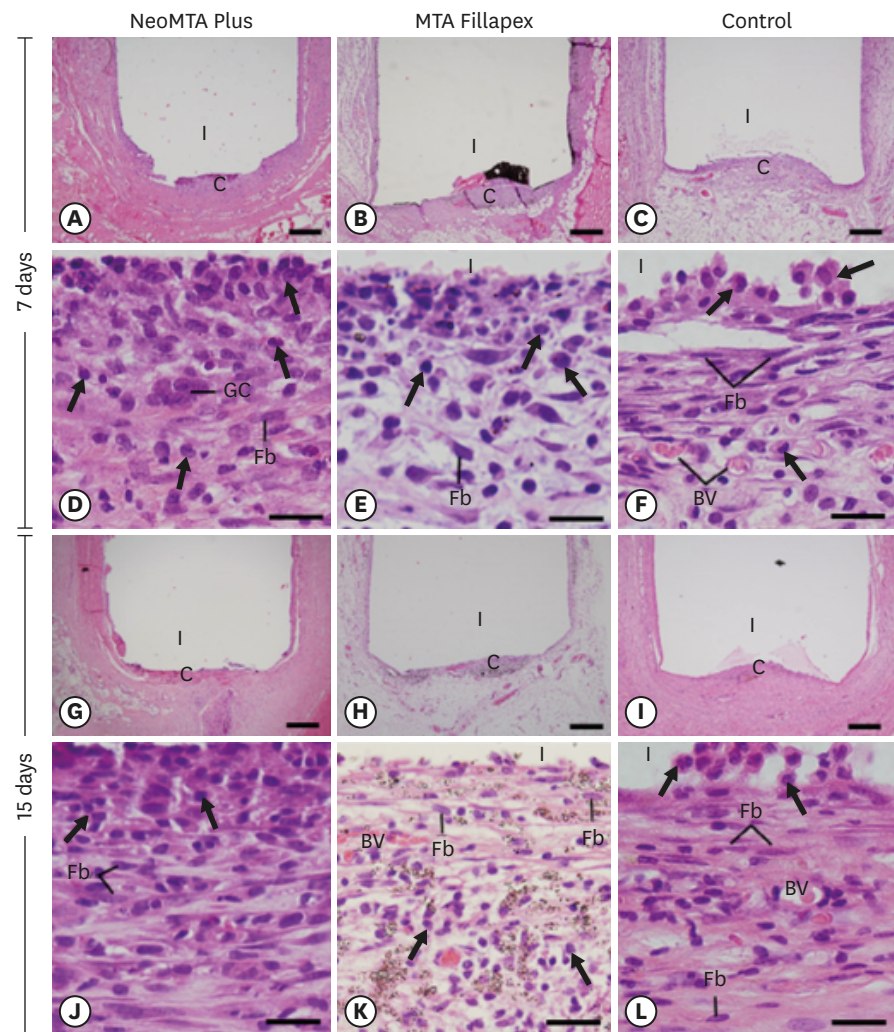


Figure 1. Light micrographs of sections of capsules at 7 days (A-F) and 15 days (G-L). (A-C and G-I) Photomicrographs at a low magnification show well-defined capsules around the implants (bars = 500 μ m). (D-F and J-L) Higher magnification of (A-C and G-I), showing inflammatory cells (arrows) and Fb (bars = 20 μ m). In MTA Fillapex (K), several material particles are seen. BV, blood vessel; C, capsules; Fb, fibroblasts; GC, multinucleated giant cell; I, space of polyethylene tubes; MTA, mineral trioxide aggregate.

polyethylene tubes (**Figure 1L**). At 30 days, the capsules in the NeoMTA Plus group (**Figure 2A**) and CG (**Figure 2C**) were thinner than those in the MTA Fillapex group (**Figure 2B**). However, under high magnification, the capsules around both sealers exhibited moderate amounts of inflammatory infiltrate (**Figure 2D and 2E**), while the capsules of the CG contained fibroblasts between collagen bundles and few ICs (**Figure 2F**). On day 60, thin capsules were present around the implants (**Figure 2G-2I**). In the NeoMTA Plus and MTA Fillapex groups (**Figure 2J and 2K**), the capsules showed a discrete inflammatory infiltrate, and small particles of material were still observed in the MTA Fillapex specimens (**Figure 2K**). In the CG, scarce macrophages were seen in the fibrous capsules (**Figure 2L**).

As shown in **Figure 2M**, the most ICs in the capsules were found in all groups on day 7. There were no significant differences ($p > 0.05$) in the number of ICs between the NeoMTA Plus and the MTA Fillapex groups after 7, 30 and 60 days. On day 15, the NeoMTA Plus specimens

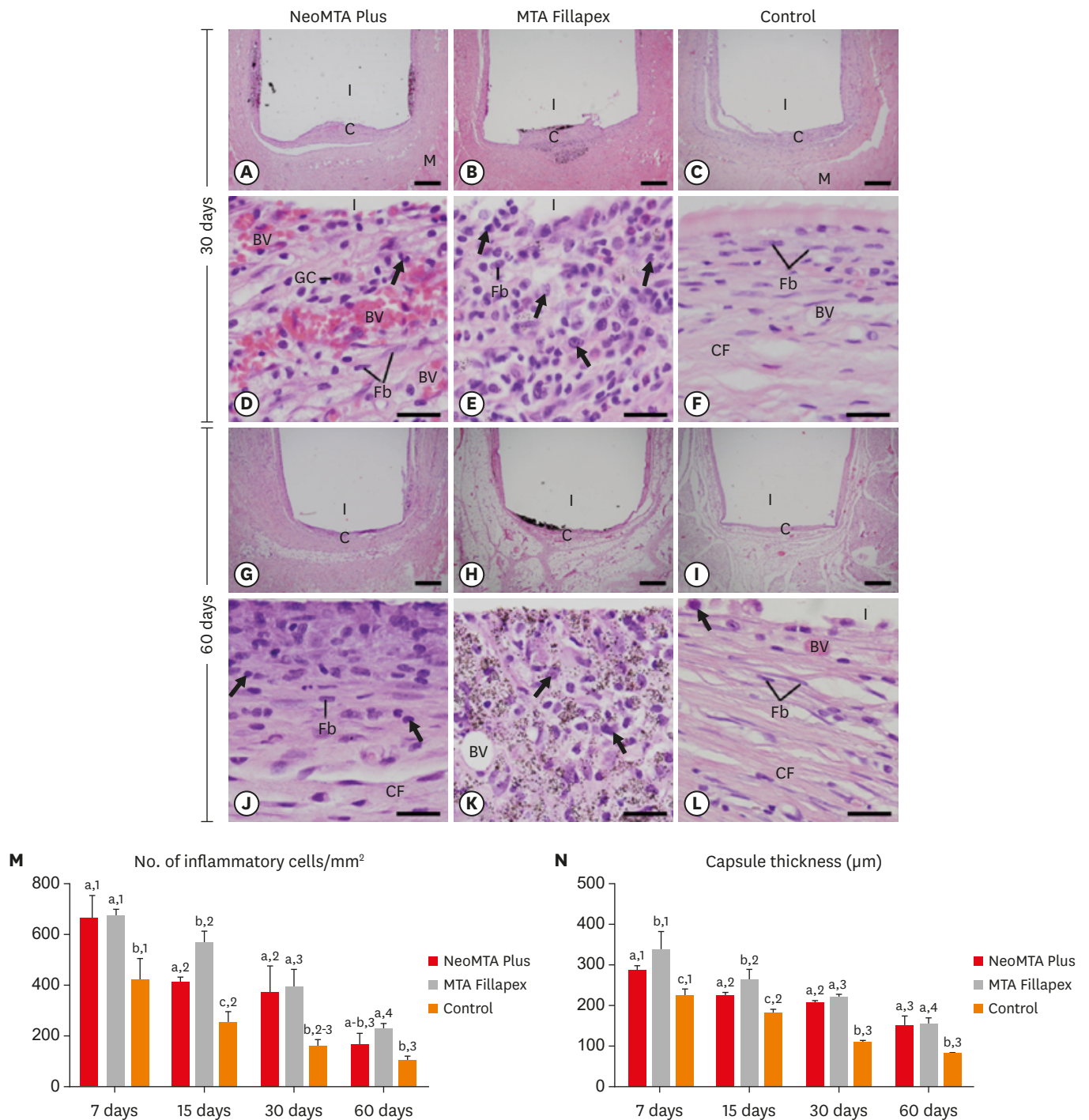


Figure 2. Light micrographs of sections of capsules at 30 days (A-F) and 60 days (G-L). (A-C and G-I) Photomicrographs show a general view of the capsules juxtaposed to the opening of the tubes. All groups exhibited thinner capsules at 60 days than at 30 days (bars = 500 μm). (D-F and J-L) Inflammatory cells (arrows) and Fb (bars = 20 μm). Note that in the control group (F and L), the capsules exhibited Fb dispersed among CF and few inflammatory cells (arrows). In MTA Fillapex (K), material particles were observed throughout the capsule. Graphs show data on the numerical density of inflammatory cells (M) and the capsule thickness (N) of the NeoMTA Plus, MTA Fillapex, and control groups at 7, 15, 30 and 60 days. Superscript letters indicate comparisons among the groups; different letters denote significant differences. Superscript numbers indicate the analysis of each group over time; different numbers denote significant differences. Tukey's test ($p \leq 0.05$). BV, blood vessel; C, capsules; CF, collagen fibers; Fb, fibroblasts; GC, multinucleated giant cell; I, space of polyethylene tubes; M, muscle tissue; MTA, mineral trioxide aggregate.

showed fewer ICs than the MTA Fillapex specimens ($p = 0.0002$). At all-time points, the CG specimens exhibited the fewest ICs. At 60 days, no significant difference was detected between the CG and NeoMTA Plus specimens ($p = 0.1137$). In all groups, the number of ICs decreased significantly over time.

As shown in **Figure 2N**, the thickness of the capsules decreased significantly over time in all groups. At 7 and 15 days, the capsules around the NeoMTA Plus specimens were significantly thinner ($p < 0.05$) than those in the MTA Fillapex specimens. However, no significant difference was found between the root canal sealers at 30 ($p = 0.5649$) and 60 ($p = 0.9162$) days. At all-time points, the CG specimens had significantly thinner capsules than were found in the NeoMTA Plus ($p \leq 0.0011$) and MTA Fillapex groups ($p < 0.0001$).

IL-6

In all groups, the capsules showed evident immunolabeling in the ICs and fibroblasts. However, a distinct pattern in the immunostaining was noticed among the groups and over time (**Figure 3A-3L**). The capsules in the MTA Fillapex group exhibited strong immunostaining, particularly at 7, 15, and 30 days (**Figure 3B, 3E, and 3H**), when compared with the NeoMTA Plus group (**Figure 3A, 3D, 3G, and 3J**) and the CG (**Figure 3C, 3F, 3I, and 3L**). Subtle immunostaining was observed in the CG specimens (**Figure 3C, 3F, 3I, and 3L**).

As shown in **Figure 3M**, the lowest number of IL-6-immunolabeled cells was observed in the CG ($p \geq 0.0306$) at all time points. At 7 and 60 days, the immunoexpression in the NeoMTA Plus group was significantly lower than in the MTA Fillapex group ($p = 0.0353$), while significant differences were not detected at 15 ($p = 0.3915$) and 30 days ($p = 0.9817$). In all groups, the immunostaining decreased significantly from 7 to 15 days ($p < 0.0001$). From 15 to 30 days, a significant reduction was detected in the MTA Fillapex group ($p = 0.0192$) and in the CG ($p = 0.0024$), whereas a significant difference was not detected in the NeoMTA Plus group ($p = 0.2392$). A significant decrease was found in the number of immunolabeled cells in the NeoMTA Plus group, the MTA Fillapex group ($p < 0.0001$), and in the CG ($p = 0.0405$) at 60 days when compared with 30 days.

Collagen content

The specimens in all groups showed an accentuated variability in the birefringence pattern, particularly over time (**Figure 4A-4L**). At 7 and 15 days, the capsules of all groups exhibited little birefringent collagen (**Figure 4A-4F**). Otherwise, the capsules of all groups showed an intricate network of birefringent collagen fibers at 30 and 60 days after implantation (**Figure 4G-4L**).

According to **Figure 4M**, the amount of birefringent material increased in all groups over time. At all-time points, there were no significant differences between NeoMTA Plus and MTA Fillapex ($p \geq 0.753$). At 7 and 15 days, no significant differences were observed among the NeoMTA group, MTA Fillapex group, and the CG. The CG exhibited greater collagen content than the MTA Fillapex ($p = 0.0472$) and NeoMTA groups ($p = 0.0368$) at 30 and 60 days, respectively.

von Kossa reaction and unstained sections analyzed by polarized light microscopy

The capsules around the NeoMTA Plus (**Figure 5A and 5B**) and MTA Fillapex (**Figure 5C and 5D**) specimens exhibited von Kossa-positive structures (black color). In the CG, von Kossa-positive structures were not seen (**Figure 5E and 5F**). Deparaffinized and unstained sections

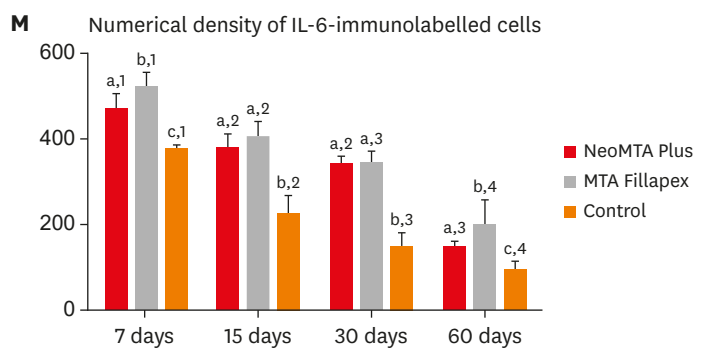
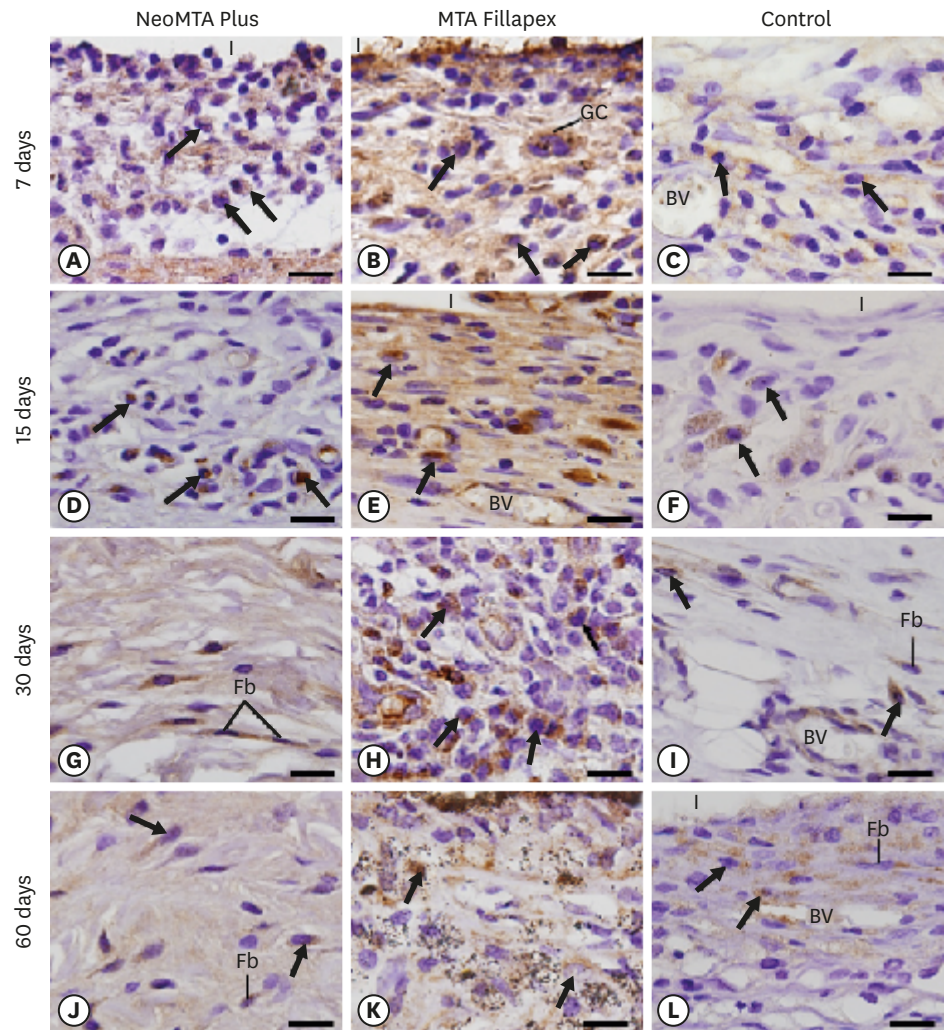


Figure 3. Light micrographs show portions of capsules juxtaposed with the implant tubes. (A-L) Immunohistochemistry was used to detect IL-6 with hematoxylin counterstaining. The immunostaining (brown-yellow color) is seen in inflammatory cells (arrows) and Fb in the capsules at all periods (bars = 20 μm). (M) Graph showing the numerical density of IL-6-immunostained cells in the NeoMTA Plus, MTA Fillapex, and control groups at 7, 15, 30, and 60 days. Superscript letters indicate comparisons among the groups; different letters denote significant differences. Subscript numbers indicate the analysis of each group over time; different numbers denote significant differences. Tukey's test ($p \leq 0.05$). BV, blood vessel; Fb, fibroblasts; GC, multinucleated giant cell; I, space of polyethylene tubes; IL, interleukin; MTA, mineral trioxide aggregate.

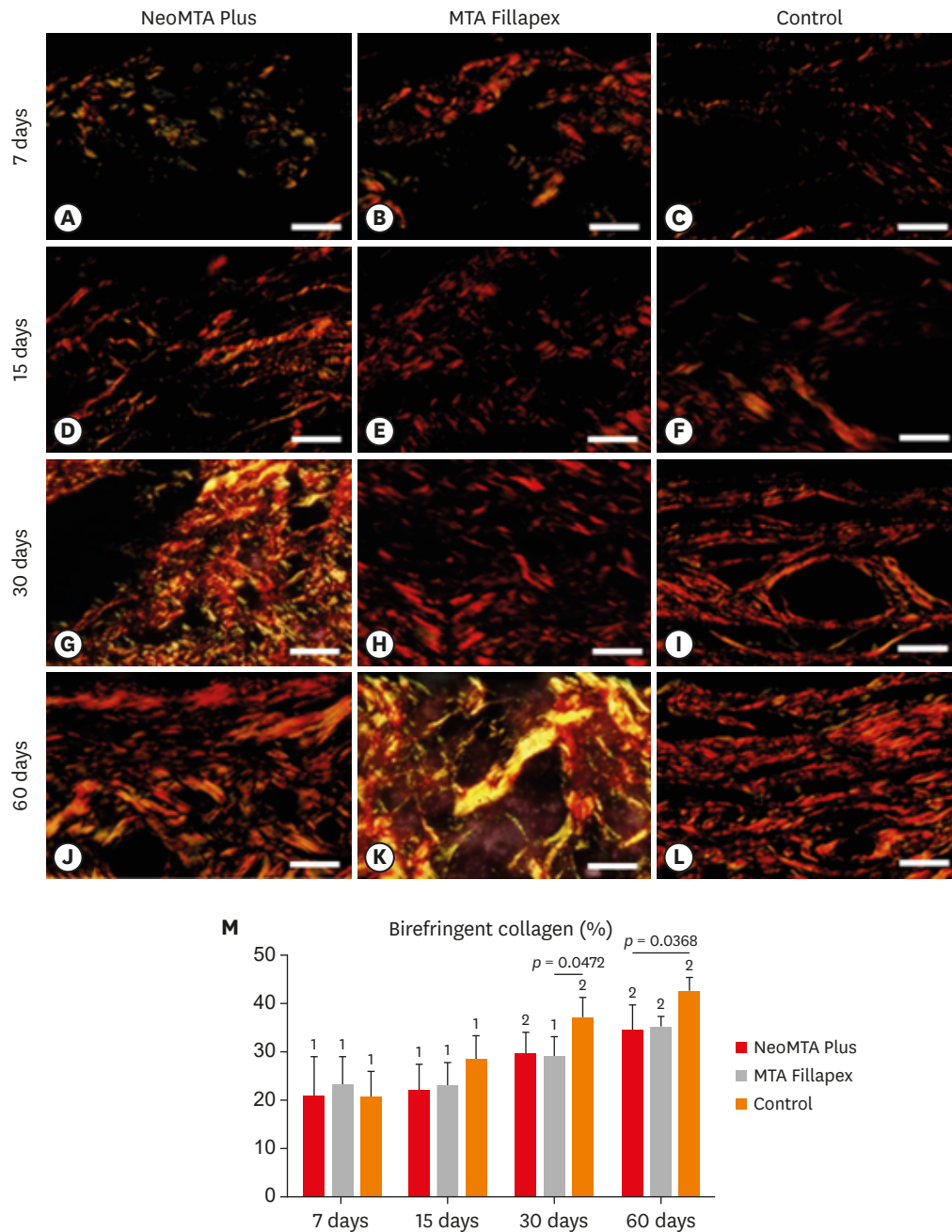


Figure 4. Light micrographs of portions of capsules juxtaposed with the implant tubes. The sections were stained with picosirius red and photographed with a polarization microscope. At 7 (A-C) and 15 (D-F) days, the capsules contained few birefringent fibers (orange/red colors). At 30 (G-I) and 60 (J-L) days, the capsules contained thick bundles of collagen exhibiting strong birefringence (bars = 20 μ m). (M) Graph illustrating the birefringent collagen content (in percentage) in NeoMTA Plus, MTA Fillapex, and control groups at 7, 15, 30, and 60 days. Superscript asterisks denote significant between-group differences. Superscript numbers indicate the analysis of each group over time; different numbers denote significant differences. Tukey's test ($p \leq 0.05$).

analyzed with polarization microscopy presented birefringent material in the capsules around the NeoMTA Plus (**Figure 5G** and **5H**) and MTA Fillapex (**Figure 5I** and **5J**) specimens.

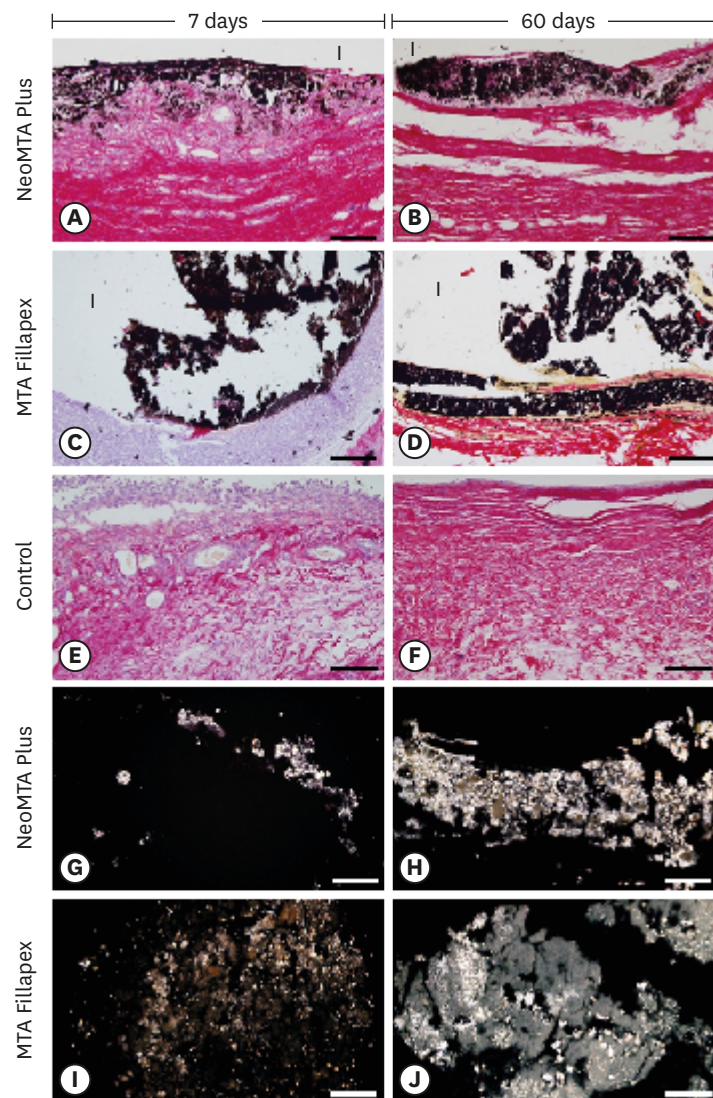


Figure 5. Light micrographs of portions of capsules juxtaposed with the implant tubes. (A-F) von Kossa histochemical reaction (black) and counterstaining with picosirius red (red). The capsules in the NeoMTA Plus and MTA Fillapex groups exhibited reactivity to the von Kossa method (structures shown in black). In the control group (E and F), von Kossa-positive structures are absent. (G-J) Unstained sections analyzed under polarized light. Fine granular material exhibiting birefringence is observed in the capsules of NeoMTA Plus and MTA Fillapex (bars = 20 μ m).

DISCUSSION

In the present study, quantitative analyses of the inflammatory reaction and IL-6-immunoreactivity indicated that NeoMTA Plus and MTA Fillapex developed a favorable tissue response over time. This explanation is supported by the observed decrease in the inflammatory reaction and in the immunoexpression of IL-6, which occurred concomitantly with the increase in the amount of collagen in the connective tissue surrounding the NeoMTA Plus and MTA Fillapex specimens over time.

NeoMTA Plus contains a fine powder of tricalcium silicate (alite), dicalcium silicate (belite), calcium sulfate (as an anhydrite), and a low amount of calcite, probably due to some storage

hydration that facilitates calcium hydroxide formation [5]. Here, NeoMTA Plus was mixed with water-based gel, which provided an adequate consistency for root canal sealing [9]. NeoMTA Plus extracts added to human osteoblast-like cells (Saos-2) culture induced cell proliferation and expression of alkaline phosphatase, culminating in the formation of mineralized nodules [12]. Another *in vitro* study using NeoMTA Plus as dental pulp capping material reported no cytotoxic effect on human dental pulp stem cells [1]. However, *in vivo* studies of NeoMTA Plus prepared as a canal root sealer, with an emphasis on its biocompatibility and bioactivity, have not been published.

NeoMTA Plus and MTA Fillapex induced a moderate inflammatory reaction in the connective tissue on day 7 after implantation, as revealed by morphological and quantitative analyses. Although both sealers promoted a moderate inflammatory infiltrate, the intensity of the reaction around endodontic sealers was approximately two-fold higher than that found in the capsules of the control group. It is possible that the higher values found in the connective tissue around the sealers may be explained, at least in part, by the alkaline pH provided by both the NeoMTA Plus and MTA Fillapex sealers. From the first 3 hours until day 7, the pH varied from 11.2 to 10.8 in a solution containing NeoMTA Plus [5] and from 9.5 to 9.2 in a solution with MTA Fillapex [10]. Despite its antimicrobial effect, as is expected in root canal sealers [23,26], the alkaline pH induces IC recruitment and the release of proinflammatory cytokines, leading to an inflammatory reaction [11,18,23]. However, the release of substances from sealers may also have a deleterious effect on connective tissue components (cellular and extracellular matrix) activating the immune and inflammatory systems [17,19,20].

The highest immunoexpression of IL-6 was observed in all 3 groups at 7 days. IL-6 is a pleiotropic cytokine synthesized by a variety of cells, including monocytes/macrophages, endothelial cells, lymphocytes, and fibroblasts [19,27,28]. IL-6 participates in several biological activities, mediating immune and inflammatory responses and stimulating hematopoiesis [29]. This cytokine has proinflammatory properties, and it stimulates the secretion of chemokines and adhesion molecules by lymphocytes and the migration of neutrophils [29,30]. There is strong evidence that IL-6 acts in the initial phase of inflammatory reactions promoted by dental materials implanted into subcutaneous tissue [17-20,31]. Likewise, high levels of IL-6 are detected in acute inflammatory reactions caused by coronary artery disease [32], rheumatoid arthritis [30,33], and periodontal disease [28,34].

Although the largest amount of inflammatory infiltrate was present in MTA Fillapex specimens at 15 days, a significant difference in the immunoexpression of IL-6 was not detected between the NeoMTA Plus and MTA Fillapex groups. In fact, a statistical analysis showed that the inflammatory infiltrate decreased significantly by 15 days in the MTA Fillapex specimens in comparison with 7 days. However, this reduction was more pronounced in the NeoMTA Plus group, indicating that the chemical composition of this sealer allows faster regression of inflammatory infiltrate. It is conceivable that the high number of IL-6-immunostained cells in MTA Fillapex specimens at 7 days may be responsible for the maintenance of inflammatory infiltrate in the connective tissue, as observed at 15 days. NeoMTA Plus is a bioceramic sealer (tricalcium silicate sealer), whereas the MTA Fillapex is a resin-based sealer containing only about 13.2% of tricalcium calcium silicate [13]. This material also contains salicylate resin, a component that exhibits high cytotoxicity [31,35]. Moreover, the mixture of this resin with the tricalcium silicate in MTA Fillapex provides high flowability and a prolonged setting time and, consequently, a high solubility [13,16,31,36]. Material particles were often dispersed throughout the capsules around the MTA Fillapex

specimens, suggesting that this sealer may exhibit high solubility when in contact with body fluids. Moreover, MTA Fillapex initially induced a more extensive inflammatory reaction since the capsules of the MTA Fillapex specimens were significantly thicker than those of NeoMTA Plus at 7 and 15 days. However, significant differences in the thickness of capsules around the endodontic sealers were not detected at 30 and 60 days. Furthermore, the thickness of capsules in these groups reached values around 150 μm ; as such, they were considered to be thin capsules [37], reinforcing the idea that these sealers are biocompatible [17,20,23].

Despite the differences in composition and physicochemical properties between NeoMTA Plus and MTA Fillapex, both root canal sealers allowed a reduction in inflammatory infiltrate and immunoexpression of IL-6 in parallel with a gradual increase in collagen, culminating in the formation of thin fibrous capsules by 60 days. Thus, NeoMTA Plus and MTA Fillapex caused transitory deleterious changes to the connective tissue, which gradually recovered, indicating that these sealers provide favorable conditions to the host cells for tissue repair.

The von Kossa method is a histochemical reaction that detects the deposition of calcium ions and is widely used to investigate the bioactivity of dental materials [2,17,23,38,39]. Structures strongly positive to the von Kossa method were seen in the connective tissue adjacent to the NeoMTA Plus and MTA Fillapex sealers suggesting that these sealers promote the calcium precipitation in the capsules. Moreover, unstained sections of NeoMTA Plus and MTA Fillapex specimens exhibited birefringent structures indicative of amorphous calcite [2,38,39]. NeoMTA Plus and MTA Fillapex release calcium ions, which react with carbon dioxide present in the tissues to form calcium carbonate crystals, which are birefringent structures under polarized light [2,24,25,39]. Although further methodologies must be deployed to confirm whether these sealers stimulate the formation of mineralized tissue, it is important to emphasize that no von Kossa-positive or birefringent structures were observed in the CG. These findings point to the bioactive potential of both sealers (NeoMTA Plus and MTA Fillapex).

CONCLUSIONS

NeoMTA Plus and MTA Fillapex are biocompatible root canal sealers, since the initial moderate inflammatory reaction was replaced by thin fibrous capsules, pointing to a structural reorganization of the connective tissue around these sealers over time. The inflammatory reaction decreased more rapidly in the NeoMTA Plus group than in the MTA Fillapex group. Furthermore, both calcium silicate-based sealers showed bioactive potential.

ACKNOWLEDGEMENTS

The authors thank Mr. Pedro Sérgio Simões for technical assistance. We thank CAPES (Brazil) for the fellowship grants to Roberto Alameda Hoshino (code 001) and Mateus Machado Delfino (code 001).

REFERENCES

1. Tomás-Catalá CJ, Collado-González M, García-Bernal D, Oñate-Sánchez RE, Forner L, Llena C, Lozano A, Moraleda JM, Rodríguez-Lozano FJ. Biocompatibility of new pulp-capping materials NeoMTA Plus, MTA Repair HP, and biodentine on human dental pulp stem cells. *J Endod* 2018;44:126-132.
[PUBMED](#) | [CROSSREF](#)
2. Cintra LTA, Benetti F, de Azevedo Queiroz ÍO, de Araújo Lopes JM, Penha de Oliveira SH, Sivieri Araújo G, Gomes-Filho JE. Cytotoxicity, biocompatibility, and biom mineralization of the new high-plasticity MTA Material. *J Endod* 2017;43:774-778.
[PUBMED](#) | [CROSSREF](#)
3. Mondelli JAS, Hoshino RA, Weckwerth PH, Cerri PS, Leonardo RT, Guerreiro-Tanomaru JM, Tanomaru-Filho M, da Silva GF. Biocompatibility of mineral trioxide aggregate flow and biodentine. *Int Endod J* 2019;52:193-200.
[PUBMED](#) | [CROSSREF](#)
4. Parirokh M, Torabinejad M, Dummer PMH. Mineral trioxide aggregate and other bioactive endodontic cements: an updated overview - Part I: Vital pulp therapy. *Int Endod J* 2018;51:177-205.
[PUBMED](#) | [CROSSREF](#)
5. Siboni F, Taddei P, Prati C, Gandolfi MG. Properties of NeoMTA Plus and MTA Plus cements for endodontics. *Int Endod J* 2017;50 Supplement 2:e83-e94.
[PUBMED](#) | [CROSSREF](#)
6. Slompo C, Peres-Buzalaf C, Gasque KC, Damante CA, Ordinola-Zapata R, Duarte MA, de Oliveira RC. Experimental calcium silicate-based cement with and without zirconium oxide modulates fibroblasts viability. *Braz Dent J* 2015;26:587-591.
[PUBMED](#) | [CROSSREF](#)
7. Bozeman TB, Lemon RR, Eleazer PD. Elemental analysis of crystal precipitate from gray and white MTA. *J Endod* 2006;32:425-428.
[PUBMED](#) | [CROSSREF](#)
8. Torabinejad M, Parirokh M. Mineral trioxide aggregate: a comprehensive literature review - Part II: Leakage and biocompatibility investigations. *J Endod* 2010;36:190-202.
[PUBMED](#) | [CROSSREF](#)
9. McMichael GE, Primus CM, Opperman LA. Dentinal tubule penetration of tricalcium silicate sealers. *J Endod* 2016;42:632-636.
[PUBMED](#) | [CROSSREF](#)
10. Siboni F, Taddei P, Zamparini F, Prati C, Gandolfi MG. Properties of BioRoot RCS, a tricalcium silicate endodontic sealer modified with povidone and polycarboxylate. *Int Endod J* 2017;50 Supplement 2:e120-e136.
[PUBMED](#) | [CROSSREF](#)
11. Quintana RM, Jardine AP, Grechi TR, Grazziotin-Soares R, Ardenghi DM, Scarparo RK, Grecca FS, Kopper PMP. Bone tissue reaction, setting time, solubility, and pH of root repair materials. *Clin Oral Investig* 2019;23:1359-1366.
[PUBMED](#) | [CROSSREF](#)
12. Tanomaru-Filho M, Andrade AS, Rodrigues EM, Viola KS, Faria G, Camilleri J, Guerreiro-Tanomaru JM. Biocompatibility and mineralized nodule formation of NeoMTA Plus and an experimental tricalcium silicate cement containing tantalum oxide. *Int Endod J* 2017;50 Supplement 2:e31-e39.
[PUBMED](#) | [CROSSREF](#)
13. Prüllage RK, Urban K, Schäfer E, Dammaschke T. Material properties of a tricalcium silicate-containing, a mineral trioxide aggregate-containing, and an epoxy resin-based root canal sealer. *J Endod* 2016;42:1784-1788.
[PUBMED](#) | [CROSSREF](#)
14. Collado-González M, García-Bernal D, Oñate-Sánchez RE, Ortolani-Seltenerich PS, Lozano A, Forner L, Llena C, Rodríguez-Lozano FJ. Biocompatibility of three new calcium silicate-based endodontic sealers on human periodontal ligament stem cells. *Int Endod J* 2017;50:875-884.
[PUBMED](#) | [CROSSREF](#)
15. Camilleri J, Montesin FE, Papaioannou S, McDonald F, Pitt Ford TR. Biocompatibility of two commercial forms of mineral trioxide aggregate. *Int Endod J* 2004;37:699-704.
[PUBMED](#) | [CROSSREF](#)
16. Tanomaru-Filho M, Cristine Prado M, Torres FFE, Viapiana R, Pivoto-João MMB, Guerreiro-Tanomaru JM. Physicochemical properties and bioactive potential of a new epoxy resin-based root canal sealer. *Braz Dent J* 2019;30:563-568.
[PUBMED](#) | [CROSSREF](#)

17. Delfino MM, Guerreiro-Tanomaru JM, Tanomaru-Filho M, Sasso-Cerri E, Cerri PS. Immunoinflammatory response and bioactive potential of GuttaFlow bioseal and MTA Fillapex in the rat subcutaneous tissue. *Sci Rep* 2020;10:7173.
[PUBMED](#) | [CROSSREF](#)
18. Silva GF, Tanomaru-Filho M, Bernardi MI, Guerreiro-Tanomaru JM, Cerri PS. Niobium pentoxide as radiopacifying agent of calcium silicate-based material: evaluation of physicochemical and biological properties. *Clin Oral Investig* 2015;19:2015-2025.
[PUBMED](#) | [CROSSREF](#)
19. da Fonseca TS, da Silva GF, Tanomaru-Filho M, Sasso-Cerri E, Guerreiro-Tanomaru JM, Cerri PS. *In vivo* evaluation of the inflammatory response and IL-6 immunoeexpression promoted by biodentine and MTA Angelus. *Int Endod J* 2016;49:145-153.
[PUBMED](#) | [CROSSREF](#)
20. Saraiva JA, da Fonseca TS, da Silva GF, Sasso-Cerri E, Guerreiro-Tanomaru JM, Tanomaru-Filho M, Cerri PS. Reduced interleukin-6 immunoeexpression and birefringent collagen formation indicate that MTA Plus and MTA Fillapex are biocompatible. *Biomed Mater* 2018;13:035002.
[PUBMED](#) | [CROSSREF](#)
21. de Pizzol Júnior JP, Sasso-Cerri E, Cerri PS. Matrix metalloproteinase-1 and acid phosphatase in the degradation of the lamina propria of eruptive pathway of rat molars. *Cells* 2018;7:e206.
[PUBMED](#) | [CROSSREF](#)
22. Silva GF, Guerreiro-Tanomaru JM, da Fonseca TS, Bernardi MIB, Sasso-Cerri E, Tanomaru-Filho M, Cerri PS. Zirconium oxide and niobium oxide used as radiopacifiers in a calcium silicate-based material stimulate fibroblast proliferation and collagen formation. *Int Endod J* 2017;50 Supplement 2:e95-e108.
[PUBMED](#) | [CROSSREF](#)
23. Hoshino RA, Silva GF, Delfino MM, Guerreiro-Tanomaru JM, Tanomaru-Filho M, Sasso-Cerri E, Filho IB, Cerri PS. Physical properties, antimicrobial activity and *in vivo* tissue response to Apexit Plus. *Materials (Basel)* 2020;13:E1171.
[PUBMED](#) | [CROSSREF](#)
24. Holland R, de Souza V, Nery MJ, Otoboni Filho JA, Bernabé PF, Dezan Júnior E. Reaction of rat connective tissue to implanted dentin tubes filled with mineral trioxide aggregate or calcium hydroxide. *J Endod* 1999;25:161-166.
[PUBMED](#) | [CROSSREF](#)
25. Gomes-Filho JE, Watanabe S, Bernabé PF, de Moraes Costa MT. A mineral trioxide aggregate sealer stimulated mineralization. *J Endod* 2009;35:256-260.
[PUBMED](#) | [CROSSREF](#)
26. Arias-Moliz MT, Camilleri J. The effect of the final irrigant on the antimicrobial activity of root canal sealers. *J Dent* 2016;52:30-36.
[PUBMED](#) | [CROSSREF](#)
27. Li Y, Chi L, Stechschulte DJ, Dileepan KN. Histamine-induced production of interleukin-6 and interleukin-8 by human coronary artery endothelial cells is enhanced by endotoxin and tumor necrosis factor-alpha. *Microvasc Res* 2001;61:253-262.
[PUBMED](#) | [CROSSREF](#)
28. de Oliveira PA, de Pizzol-Júnior JP, Longhini R, Sasso-Cerri E, Cerri PS. Cimetidine reduces interleukin-6, matrix metalloproteinases-1 and -9 immunoeexpression in the gingival mucosa of rat molars with induced periodontal disease. *J Periodontol* 2017;88:100-111.
[PUBMED](#) | [CROSSREF](#)
29. Kang S, Tanaka T, Narazaki M, Kishimoto T. Targeting interleukin-6 signaling in clinic. *Immunity* 2019;50:1007-1023.
[PUBMED](#) | [CROSSREF](#)
30. Hashizume M, Mihara M. The roles of interleukin-6 in the pathogenesis of rheumatoid arthritis. *Arthritis (Egypt)* 2011;2011:765624.
[PUBMED](#) | [CROSSREF](#)
31. Silva EJ, Rosa TP, Herrera DR, Jacinto RC, Gomes BP, Zaia AA. Evaluation of cytotoxicity and physicochemical properties of calcium silicate-based endodontic sealer MTA Fillapex. *J Endod* 2013;39:274-277.
[PUBMED](#) | [CROSSREF](#)
32. James SK, Oldgren J, Lindbäck J, Johnston N, Siegbahn A, Wallentin L. An acute inflammatory reaction induced by myocardial damage is superimposed on a chronic inflammation in unstable coronary artery disease. *Am Heart J* 2005;149:619-626.
[PUBMED](#) | [CROSSREF](#)

33. Narazaki M, Tanaka T, Kishimoto T. The role and therapeutic targeting of IL-6 in rheumatoid arthritis. *Expert Rev Clin Immunol* 2017;13:535-551.
[PUBMED](#) | [CROSSREF](#)
34. Noh MK, Jung M, Kim SH, Lee SR, Park KH, Kim DH, Kim HH, Park YG. Assessment of IL-6, IL-8 and TNF- α levels in the gingival tissue of patients with periodontitis. *Exp Ther Med* 2013;6:847-851.
[PUBMED](#) | [CROSSREF](#)
35. Poggio C, Riva P, Chiesa M, Colombo M, Pietrocola G. Comparative cytotoxicity evaluation of eight root canal sealers. *J Clin Exp Dent* 2017;9:e574-e578.
[PUBMED](#) | [CROSSREF](#)
36. Vitti RP, Prati C, Silva EJ, Sinhoreti MA, Zanchi CH, de Souza e Silva MG, Ogliari FA, Piva E, Gandolfi MG. Physical properties of MTA Fillapex sealer. *J Endod* 2013;39:915-918.
[PUBMED](#) | [CROSSREF](#)
37. Yaltirik M, Ozbas H, Bilgic B, Issever H. Reactions of connective tissue to mineral trioxide aggregate and amalgam. *J Endod* 2004;30:95-99.
[PUBMED](#) | [CROSSREF](#)
38. Cintra LT, Ribeiro TA, Gomes-Filho JE, Bernabé PF, Watanabe S, Facundo AC, Samuel RO, Dezan-Júnior E. Biocompatibility and biomineralization assessment of a new root canal sealer and root-end filling material. *Dent Traumatol* 2013;29:145-150.
[PUBMED](#) | [CROSSREF](#)
39. Bueno CR, Valentim D, Marques VA, Gomes-Filho JE, Cintra LT, Jacinto RC, Dezan-Junior E. Biocompatibility and biomineralization assessment of bioceramic-, epoxy-, and calcium hydroxide-based sealers. *Braz Oral Res* 2016;30:e81.
[PUBMED](#) | [CROSSREF](#)